ORIGINAL ARTICLE

Journal of Cachexia, Sarcopenia and Muscle 2022; **13**: 1210–1223
Published online 9 February 2022 in Wiley Online Library (wileyonlinelibrary.com) **DOI:** 10.1002/jcsm.12929

m^{6}A demethylase ALKBH5 drives denervation-induced muscle atrophy by targeting HDAC4 to activate FoxO3 signalling

Yuantong Liu[1,2*], Tianjian Zhou[1], Qinghe Wang[1], Runhan Fu[2], Zengfu Zhang[2], Nandi Chen[1], Zhizhong Li[3*], Guoyong Gao[1*], Songlin Peng[1*] & Dazhi Yang[1*]

[1]*Department of Spine Surgery, Shenzhen People's Hospital, The Second Clinical Medical College, Jinan University, Shenzhen, China;* [2]*Department of Orthopedics, Qilu Hospital of Shandong University, Jinan, China;* [3]*The First Affiliated Hospital, Jinan University, Guangzhou, China*

Abstract

Background Skeletal muscle atrophy is a common clinical manifestation of various neurotrauma and neurological diseases. In addition to the treatment of primary neuropathies, it is a clinical condition that should be investigated. FoxO3 activation is an indispensable mechanism in denervation-induced muscle atrophy; however, upstream factors that control FoxO3 expression and activity have not been fully elucidated. N^6-methyladenosine (m^{6}A) methylation is a novel mode of epitranscriptional gene regulation that affects several cellular processes. However, the biological significance of m^{6}A modification in FoxO3-dependent atrophy is unknown.

Methods We performed gain-of-function and loss-of-function experiments and used denervation-induced muscle atrophy mouse model to evaluate the effects of m^{6}A modification on muscle mass control and FoxO3 activation. m^{6}A-sequencing and mass spectrometry analyses were used to establish whether histone deacetylase 4 (HDAC4) is a mediator of m^{6}A demethylase ALKBH5 regulation of FoxO3. A series of cellular and molecular biological experiments (western blot, immunoprecipitation, half-life assay, m^{6}A-MeRIP-qPCR, and luciferase reporter assays among others) were performed to investigate regulatory relationships among ALKBH5, HDAC4, and FoxO3.

Results In skeletal muscles, denervation was associated with a 20.7–31.9% decrease in m^{6}A levels ($P < 0.01$) and a 35.6–115.2% increase in demethylase ALKBH5 protein levels ($P < 0.05$). Overexpressed ALKBH5 reduced m^{6}A levels, activated FoxO3 signalling, and induced excess loss in muscle wet weight (−10.3% for innervation and −11.4% for denervation, $P < 0.05$) as well as a decrease in myofibre cross-sectional areas (−35.8% for innervation and −33.3% for denervation, $P < 0.05$) during innervation and denervation. Specific deletion of *Alkbh5* in the skeletal muscles prevented FoxO3 activation and protected mice from denervation-induced muscle atrophy, as evidenced by increased muscle mass (+16.0%, $P < 0.05$), size (+50.0%, $P < 0.05$) and MyHC expression (+32.6%, $P < 0.05$). Mechanistically, HDAC4 was established to be a crucial central mediator for ALKBH5 in enhancing FoxO3 signalling in denervated muscles. ALKBH5 demethylates and stabilizes *Hdac4* mRNA. HDAC4 interacts with and deacetylates FoxO3, resulting in a significant increase in FoxO3 expression (+61.3–82.5%, $P < 0.01$) and activity (+51.6–122.0%, $P < 0.001$).

Conclusions Our findings elucidate on the roles and mechanisms of ALKBH5-mediated m^{6}A demethylation in the control of muscle mass during denervation and activation of FoxO3 signalling by targeting HDAC4. These results suggest that ALKBH5 is a potential therapeutic target for neurogenic muscle atrophy.

Keywords Muscle atrophy; Denervation; FoxO3; m^{6}A modification; ALKBH5; HDAC4

Received: 30 June 2021; Revised: 26 November 2021; Accepted: 28 December 2021
**Correspondence to: Yuantong Liu, Department of Orthopedics, Qilu Hospital of Shandong University, 44 Wenhua Xi Road, Jinan, 250012, China. Email: liuytog@gmail.com. Dazhi Yang, Songlin Peng, Guoyong Gao, Department of Spine Surgery, Shenzhen People's Hospital, The Second Clinical Medical College, Jinan University, 1017 Dongmen Bei Road, Shenzhen 518020, China. Email: yangdazhi1111@163.com; dyffyy2@mail.sustech.edu.cn; guoyonggao@hotmail.com. Zhizhong Li, The First Affiliated Hospital, Jinan*

University, 613 West Huangpu Avenue, Guangzhou, 510630, China. Email: lizhizhongjd@163.com

Introduction

The skeletal muscle is the final executive organ of the human body for voluntary movement and postural support. Maintenance of its morphological structure and functional state depends on normal motor nerve innervation. However, under various pathological conditions, such as peripheral nerve injury, motor neuron and neuromuscular junction diseases, normal nerve signal transduction and neuronutritional supply of skeletal muscles are disturbed. Therefore, patients suffer from severe progressive muscle mass loss and weakness, known as denervation-induced muscle atrophy.[1] Notably, nerve repair takes a long time. Primary neuropathy treatment does not significantly alleviate the problem as the muscle structure is seriously damaged due to long denervation periods. Therefore, the original shape and function of muscle fibres are not restored after they regain motor nerve signals. This implies that prevention of muscle atrophy is challenging in addition to treatment of primary neuropathy. Currently, due to the lack of a deep understanding of the regulatory mechanisms of skeletal muscle mass, there are no effective measures for preventing neurogenic muscle atrophy.

Overactivation of the ubiquitin-proteasome proteolytic system is a major cellular process that results in denervation-induced muscle atrophy,[2,3] and its activation is significantly correlated with upregulation of atrophy-related genes (atrogenes), including *Atrogin1*, *MuRF1*, *MUSA1*, *SMART*.[4,5] Moreover, the transcription factor FoxO3, a member of Forkhead box (Fox) family, plays an important role in regulation of atrogene expression. FoxO3 binds promoter regions and activates atrogene transcription, resulting in the occurrence and progression of skeletal muscle atrophy induced by various pathological states.[5–8] However, as a human longevity gene, inhibition of FoxO3 activity increases the risk of age-associated diseases.[9] Notably, development of inhibitors with the ability to target transcription factors is complex and challenging.[10] Therefore, studies should investigate upstream factors that regulate activation of FoxO3 signalling in denervation-induced muscle atrophy to develop alternative therapies.

Post-transcriptional modification of messenger RNA (mRNA) is a key mechanism in the control of gene expression levels. Among the more than 100 modifications in mRNA, N^6-methyladenosine (m^6A) methylation is the most characterized and abundant post-transcriptional modification in eukaryotic mRNA. In mammals, m^6A is catalysed by RNA methyltransferase-like 3 (METTL3) and methyltransferase-like 14 (METTL14) (writers), is removed by demethylases fat mass and obesity-associated protein (FTO) and alkB homologue 5 (ALKBH5) (erasers), and interacts with m^6A-binding proteins with YTH domain, such as YTHDF1/2/3, YTHDC1/2 (readers).[11] These three effectors regulate various cellular processes by dynamically modulating RNA splicing, translocation, stability, and translation efficiency.[12]

In recent years, various studies have evaluated the biological functions of m^6A methylation in mRNA. m^6A is implicated in various physiological and pathological processes, including stem cell fate determination,[13] neural development,[14] cardiac hypertrophy,[15] tumorigenesis, and metastasis.[16] Dynamic m^6A modification, mediated by METTL3 and FTO, plays an important role in promoting myogenic differentiation and muscle development.[17,18] Additionally, ALKBH5-mediated m^6A demethylation enhances FOXM1 expression in cancer cells,[19,20] suggesting that the Fox protein family is the likely potential target that is regulated by m^6A. However, it has not been determined whether m^6A is involved in the control of adult muscle mass, and whether it affects FoxO3-dependent neurogenic muscle atrophy.

In this study, we found that ALKBH5-meditaed m^6A demethylation aggravates muscle mass loss during denervation and that HDAC4/FoxO3 signalling axis is an important pathways downstream of ALKBH5. Our findings provide a more promising enzyme treatment target for neurogenic muscle atrophy.

Materials and methods

An extended materials and methods section can be found online in the Supporting information.

Generation of muscle-specific Alkbh5 knockout mice

Mice bearing the *Alkbh5*-floxed allele (*Alkbh5*$^{fl/fl}$, Cyagen) were crossed with transgenic mice expressing Cre recombinase under the control of the *Myl1* promoter (*Myl1-Cre*; Stock No: 024713, The Jackson Laboratory) to generate muscle-specific *Alkbh5* knockout mice (*Myl1-Cre*; *Alkbh5*$^{fl/fl}$). Littermate *Alkbh5*$^{fl/fl}$ mice were used as controls. Genotyping by tail DNA and PCR were performed at 4 weeks of age. The primers were shown in *Table* S1. Mice were housed under specific pathogen-free conditions at 24 ± 2 °C with a 12:12 h light–dark cycle and *ad libitum* access to food and water. All experimental animal procedures strictly adhered to the National Institutes of Health Guide for the Care and Use of Laboratory Animals and approved by Jinan University Laboratory Animal Ethics Committee (IACUC Issue No. 20200318-36).

m^{6}A sequencing (m^{6}A-seq) and data analysis

m^{6}A-seq and data analysis were performed by Shanghai Jiayin Biotechnology Ltd. Briefly, total RNA from 2 week-denervated gastrocnemius (GAS) muscle was extracted using the TRIzol reagent (Invitrogen), and fragmented into ~200-nucleotide-long fragments. Approximately 5% of the fragmented RNA was used as the input RNA. Other RNA fragments were analysed by immunoprecipitation using anti-m^{6}A polyclonal antibodies. Sequencing was performed using an Illumina NovaSeq 6000 platform. m^{6}A-seq data were analysed as previously described.[21] m^{6}A peaks with false discovery rate (FDR) < 0.05 were detected using transcriptome based peak caller MetPeak, and the top 5000 peaks were chosen for *de novo* motif analysis with MEME, which takes 200-nt-long peak summit-centred sense sequences as input. Peak files of different groups were merged using the merge in bedtools toolset. Signals in two different groups on every merged m^{6}A peaks was calculated using UCSC tools. m^{6}A peaks were identified as differential peaks if they had m^{6}A enrichment score fold change (FC) ≥ 2 and average m^{6}A score greater than 6. Annotation of m^{6}A peaks on the whole genome was obtained using ChIPseeker.

Liquid chromatography–tandem mass spectrometry for determination of m^{6}A/A ratio

Approximately 500 ng of purified mRNA was digested with Nuclease P1 (1 U; Sigma) in 25 μL of reaction buffer (10 mM NaCl, 2.0 mM $ZnCl_2$) containing 10 mM NH_4OAc (pH 5.3) at 42°C for 2 h, followed by addition of NH_4HCO_3 (3 μL, 3 M) and alkaline phosphatase (1 μL, 1 U/μL; Sigma) and incubation at 37°C for 2 h. After neutralization using 1 μL HCl (3 M), samples were diluted to 50 μL and filtered (0.22 μm, Millipore). Then 5 μL of the solution was used as the injection volume for liquid chromatography–tandem mass spectrometry (LC–MS/MS). Nucleosides were separated by reverse-phase ultra-performance liquid chromatography on a C18 column (Phenomenex), followed by online mass spectrometry detection using a Thermo Fisher Q Exactive Focus Orbitrap UPLC mass spectrometer via the positive electrospray ionization mode. All nucleosides were quantified based on retention time and nucleoside-to-base ion mass transitions of 282 to 150 (m^{6}A) and 268 to 136 (A). A standard curve was generated using pure nucleoside standards running in the same batch of samples. The ratio of m^{6}A to A was calculated based on calibrated concentrations.

m^{6}A dot blot assay

After being denatured by heating at 72°C for 5 min, mRNA in a volume of 1.5 μL was spotted on Hybond Nitrocellulose Membranes (Pall) and cross-linked to the membrane by UV. One of the membranes was blocked using 5% non-fat dry milk in TBST for 1 h at room temperature and inducted with rabbit anti-m^{6}A antibody (1:3000; Synaptic Systems) overnight at 4°C. Next day, the membrane was inducted with HRP-conjugated goat anti-rabbit IgG (1:5000) for 2 h at room temperature, then visualized on GNOME XRQ NPC (Syngene) using ECL chemiluminescence (Millipore). The other membrane was stained with 0.02% methylene blue in 0.3 M sodium acetate (pH 5.2) for 2 h as the loading control.

Statistical analysis

Statistical analyses were performed using the SPSS 13.0 software. Statistically significant differences between experimental groups were determined by a two-tailed Student's *t* test or one-way analysis of variance (ANOVA) followed by Bonferroni's multiple comparisons test. Data are presented as the mean ± SD or mean ± SEM (*$P < 0.05$; **$P < 0.01$; and ***$P < 0.001$).

Results

Suppressed m^{6}A levels in denervated muscles were correlated with upregulation of ALKBH5

The LC–MS/MS and dot blot showed that m^{6}A modification levels in muscles at different days after denervation were significantly low, compared with normal muscles (*Figure* 1A). Meanwhile, suppressed m^{6}A levels correlated with increased demethylase ALKBH5 levels in denervated muscles, whereas changes in METTL3, METTL14, and FTO levels after denervation were not significant (*Figure* 1B–1E). Notably, upregulation of ALKBH5 was consistent with upregulation of FoxO3 on different days post-denervation (*Figure* 1D and 1E). These findings show a strong association between ALKBH5-mediated m^{6}A demethylation with muscle wasting and FoxO3 expression, implying that ALKBH5 plays an important role in FoxO3-dependent neurogenic muscle atrophy.

ALKBH5 overexpression induces muscle mass loss and accelerates denervation-induced muscle atrophy

To explore the potential role of ALKBH5 in muscle mass control and denervation-induced muscle atrophy, ALKBH5 was overexpressed in tibialis anterior (TA) muscles through AAV-ALKBH5 local injection. Infection with AAV-ALKBH5 efficiently increased ALKBH5 expression at mRNA and protein levels in innervated and denervated TA muscles (*Figure* 2A–2C). Dot blot analysis showed that overexpressed ALKBH5

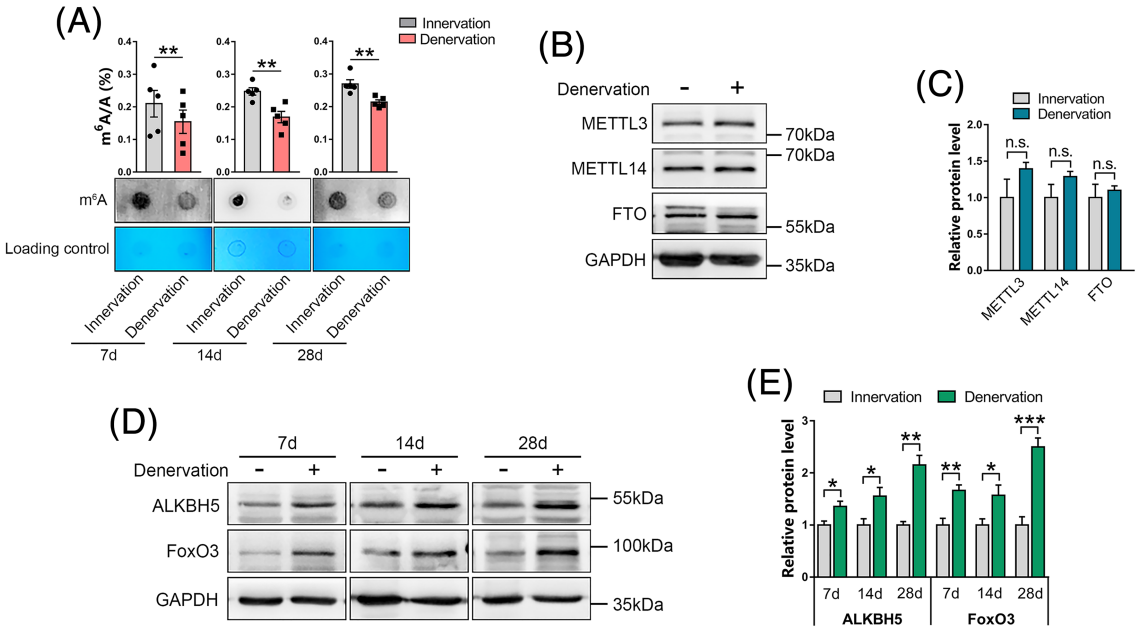

Figure 1 Decrease in m^{6}A levels in denervated muscles is accompanied by upregulation of ALKBH5. (A) m^{6}A mRNA levels in gastrocnemius (GAS) muscles on Days 7, 14, and 28 post-denervation as determined using liquid chromatography–tandem mass spectrometry (LC–MS/MS) (up) and dot-blot (down) (n = 5). (B and C) METTL3, METTL14, and FTO protein levels in innervated and denervated GAS muscles (n = 5). GAPDH was used as the internal reference. (D and E) expression and quantification of ALKBH5 and FoxO3 protein in GAS muscles at 7, 14, and 28 days post-denervation (n = 5). Data are expressed as mean ± SEM. *$P < 0.05$, **$P < 0.01$, ***$P < 0.001$, n.s., no significant by two-tailed Student's t-test.

significantly suppressed the levels of m^{6}A modifications (*Figure* 2D), thereby confirming the role of ALKBH5 as an m^{6}A "eraser" of mRNA. Notably, overexpressed ALKBH5 significantly reduced muscle wet weight (AAV-Control 59.59 ± 2.59 mg, AAV-ALKBH5 53.47 ± 3.71 mg), myofibre CSA (AAV-Control 4751.56 ± 568.24 μm^2, AAV-ALKBH5 3052.40 ± 252.78 μm^2), and MyHC expression in innervated muscles (*Figure* 2B, 2C and 2E–2I). Furthermore, overexpressed ALKBH5 was associated with excessive loss in muscle mass (AAV-Control 39.92 ± 4.20 mg, AAV-ALKBH5 35.35 ± 2.23 mg) and size (AAV-Control 3405.11 ± 487.64 μm^2, AAV-ALKBH5 2269.78 ± 289.79 μm^2) in denervated muscles (*Figure* 2E–2H and 2J). Western blot and qPCR showed that overexpressed ALKBH5 not only promoted the levels of FoxO3 and its target genes (*Atrogin1* and *MuRF1*) in TA muscles (*Figure* 2B, 2C, 2K and 2L) but also reduced the proportion of pFoxO3 (the phosphorylation status by which FoxO3 is exported from the nucleus and degraded in the cytoplasm[22]) (*Figure* S1). These findings indicate that upregulation of ALKBH5 has the ability to drive normal muscle mass loss and aggravate denervation-induced muscle atrophy by enhancing FoxO3 expression and activity.

Conditional deletion of Alkbh5 in skeletal muscles did not cause developmental defects but abrogated denervation-induced muscle atrophy

ALKBH5 overexpression was involved in initiation of muscle wasting; therefore, further experiments were performed to determine whether *Alkbh5* deletion can increase muscle mass or prevent muscle atrophy. *Alkbh5*$^{fl/+}$ mice were bred with *Myl1-Cre* transgenic mice to obtain muscle-specific *Alkbh5* knockout (*Myl1-Cre*;*Alkbh5*$^{fl/fl}$) mice, and their littermate control (*Alkbh5*$^{fl/fl}$) mice (*Figure* 3A and 3B). qPCR and western blot revealed suppressed ALKBH5 mRNA and protein levels in skeletal muscles of *Myl1-Cre*;*Alkbh5*$^{fl/fl}$ mice (*Figures* 3C, 3D, and S2A), but not in other tissues (*Figure* S2B), which subsequently elevated m^{6}A levels in denervated muscles (*Figure* 3E). *Myl1-Cre*;*Alkbh5*$^{fl/fl}$ mice were viable and did not show any morphological or growth abnormalities. Moreover, they had normal body weights (*Figure* S2C–S2E). Grip strength was comparable in the two genotypes (*Figure* S2F), and no histopathologic changes were observed in *Alkbh5* knockout muscles (*Figure* S2G). In addition, wet weight and myofibre cross-sectional area (CSA) of muscles in *Alkbh5* knockout mice at 10 weeks of age were not significantly different, compared with those in littermate controls (*Figure* 3F–3J). This implies that deletion of *Alkbh5* had no effect on normal muscle mass and function in mice. Further, the effects of *Alkbh5* deficiency on denervation-induced muscle atrophy

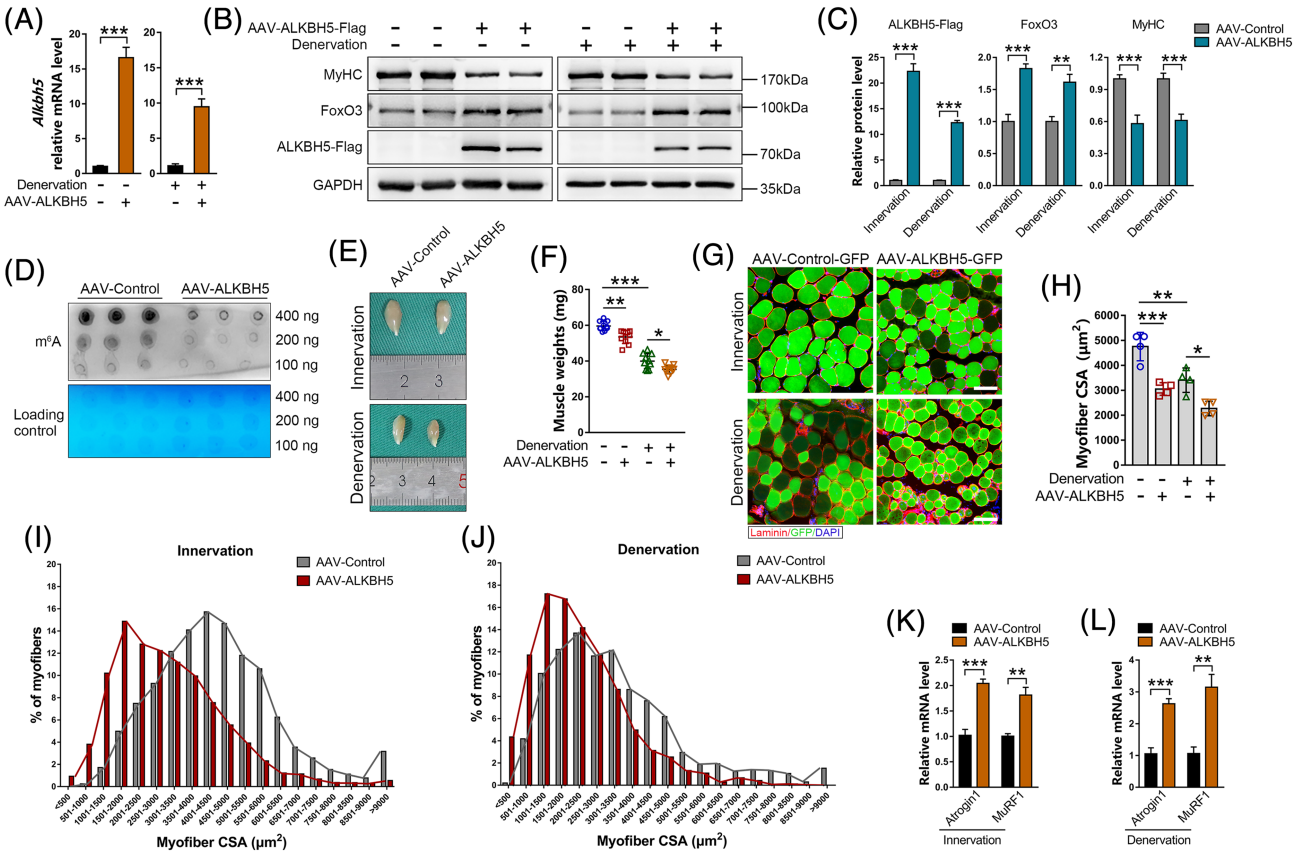

Figure 2 F ALKBH5 overexpression induces muscle mass loss and accelerates denervation-induced muscle atrophy. (A) *Alkbh5* mRNA levels after AAV-ALKBH5 injection into tibialis anterior (TA) muscle (n = 4). (B and C) MyHC, FoxO3, and ALKBH5-Flag protein levels in TA muscles after 6 weeks of AAV-ALKBH5 infection and/or two weeks of denervation (n = 6). (D) mRNA dot blot analysis of m^{6}A levels in AAV-ALKBH5 infected TA muscle. (E and F) Representative images and TA muscle wet weight after six weeks of AAV-ALKBH5 infection (n = 10). (G and H) Representative immunofluorescence images of TA muscles after AAV-ALKBH5 injection labelled with laminin (red) and GFP (green), and quantification of myofibre cross-sectional areas (CSAs) (n = 4). DAPI (blue) was used to label the nuclei. Scale bar = 100 μm. (I and J) Distribution of myofibre CSA from images in (G). (K and L) mRNA levels of *Atrogin1* and *MuRF1* in AAV-ALKBH5 infected TA muscles with innervation or denervation (n = 4). Data are expressed as mean ± SEM (A, C, K, L) or mean ± SD (F, H). *$P < 0.05$, **$P < 0.01$, ***$P < 0.001$ by two-tailed Student's t test (A, C, K, L) or one-way ANOVA with Bonferroni's post-hoc test (F, H).

were investigated. It was established that upon denervation, *Alkbh5* knockout mice exhibited larger muscle weights (control 81.39 ± 8.34 mg, knockout 94.43 ± 8.65 mg) (*Figure* 3F and 3G) and myofibre CSA (control 1103.22 ± 262.42 μm^2, knockout 1654.70 ± 376.75 μm^2) (*Figure* 3H–3K), and higher MyHC expression levels (*Figure* 3L and 3M), compared with controls. Specifically, analysis of fibre types showed that *Alkbh5* deficiency mainly inhibited type II fibres atrophy, but had no significant effect on type I fibres (*Figure* S3). This may be because the main myofibre in the GAS muscle was Type II or fast-twitch fibres.[23] Western blot and qPCR showed that *Alkbh5* knockout significantly suppressed FoxO3, *Atrogin1* and *MuRF1* levels in denervated GAS muscles, compared with the control group (*Figure* 3L–3N). These findings imply that muscle-specific *Alkbh5* knockout can prevent the activation of FoxO3 signalling and progression of muscle atrophy induced by denervation without causing muscle hypertrophy.

Identification of m^{6}A targets in denervation muscles

To establish the underlying mechanism of m^{6}A modification in regulation of neurogenic muscle atrophy, m^{6}A methylomes of skeletal muscles undergoing denervation were mapped by m^{6}A sequencing (m^{6}A-seq). The 'GGAC' sequence motif was highly enriched within the m^{6}A sites identified in both innervated and denervated muscles (*Figure* 4A), majority of the m^{6}A peaks were located in 3′UTR and CDS regions, with a small subset of peaks located in 5′UTR and distal intergenic regions (*Figure* S4A and S4B). Guitar analysis revealed that m^{6}A peaks were predominantly abundant in the vicinity of stop codons (*Figure* 4B). A total of 556 new m^{6}A peaks and 779 disappearing peaks were identified in denervated muscles through m^{6}A-seq analysis, whereas the remaining 8209 peaks were unchanged in both innervated and denervated

DOI: 10.1002/jcsm.12929

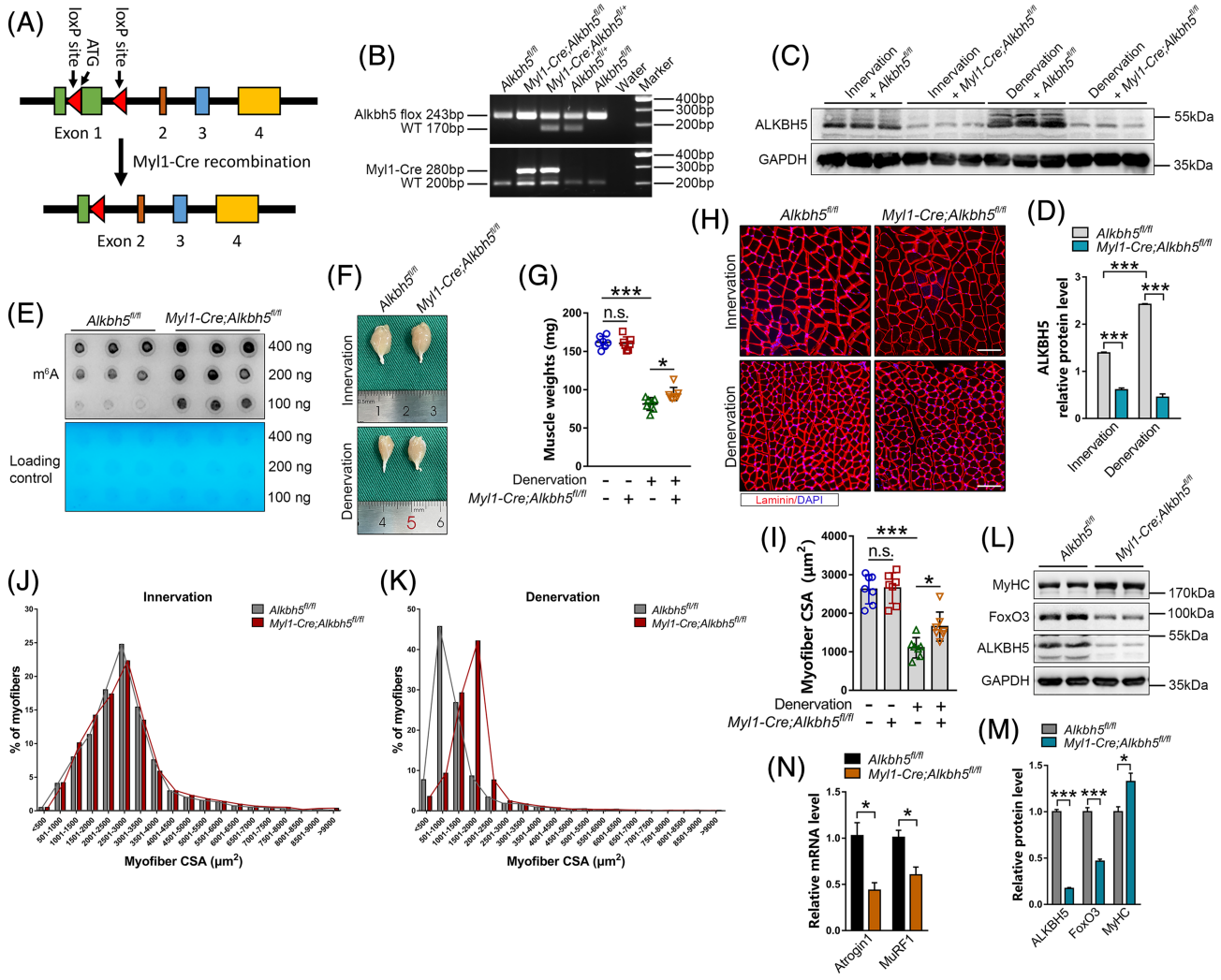

Figure 3 Conditional deletion of *Alkbh5* in skeletal muscles causes no developmental defects, but abrogates muscle atrophy induced by denervation. (A) Schematic showing generation of muscle-specific *Alkbh5* knockout mice using the Cre-LoxP recombination system. Exon 1 is deleted upon *Myl1*-Cre-mediated recombination. (B) PCR analysis with tail DNA from *Alkbh5*$^{fl/fl}$ and *Myl1-Cre;Alkbh5*$^{fl/fl}$ mice. (C–E) Western blot for ALKBH5 protein levels and dot blot for m^{6}A abundance in *Alkbh5*$^{fl/fl}$ and *Myl1-Cre;Alkbh5*$^{fl/fl}$ gastrocnemius (GAS) muscle with or without denervation (n = 3). (F and G) Representative image and GAS muscle wet weight in *Alkbh5* wild-type and knockout mice with or without denervation (n = 7). (H and I) Immunofluorescence staining and quantification of myofibre CSA of GAS muscle at 14 days post-denervation in *Alkbh5* wild-type and knockout mice (n = 7). Red denotes laminin; blue denotes nuclei labelled with DAPI. Scale bar = 100 μm. (J and K) Distribution of myofibre CSA from images in (H). (L and M) MyHC, FoxO3, and ALKBH5 protein levels in *Myl1-Cre;Alkbh5*$^{fl/fl}$ GAS muscle after 14 days of denervation (n = 6). (N) qPCR showing reduction in *Atrogin1* and *MuRF1* mRNA levels at 14 days post-denervation in muscles of *Myl1-Cre;Alkbh5*$^{fl/fl}$ mice (n = 4). Data are expressed as mean ± SEM (D, M, N) or mean ± SD (G, I). *$P < 0.05$, **$P < 0.01$, ***$P < 0.001$ by two-tailed Student's t test (D, M, N) or one-way ANOVA with Bonferroni's post-hoc test (G, I).

muscles (*Figures* 4C and S4C). For m^{6}A-regulated genes, m^{6}A-seq showed 441 new modifying genes and 621 genes loss of m^{6}A modification in denervated muscles (*Table* S2), whereas the other 3890 genes were identified in both innervated and denervated muscles (*Figure* S4D). These results demonstrate that atrophic muscles unique peaks and genes had specific m^{6}A targets.

Given that ALKBH5 promoted FoxO3 expression during denervation just at the protein level without affecting its mRNA (*Figures* 2B, 2C, and S5), we postulated that the increase in FoxO3 protein levels in denervated muscles may be caused by enhanced *FoxO3* translation efficiency through ALKBH5-mediated m^{6}A demethylation. However, m^{6}A-seq analysis showed that FoxO3 is not one of the differential genes of m^{6}A modification, implying that expressions of FoxO3 proteins in atrophic muscles are not directly regulated by m^{6}A. Consistent with this finding, a previous study reported that FoxO3 translation is independent of m^{6}A methylation.[24] Therefore, to determine how ALKBH5 regulates FoxO3 expression and muscle atrophy, we reviewed

DOI: 10.1002/jcsm.12929

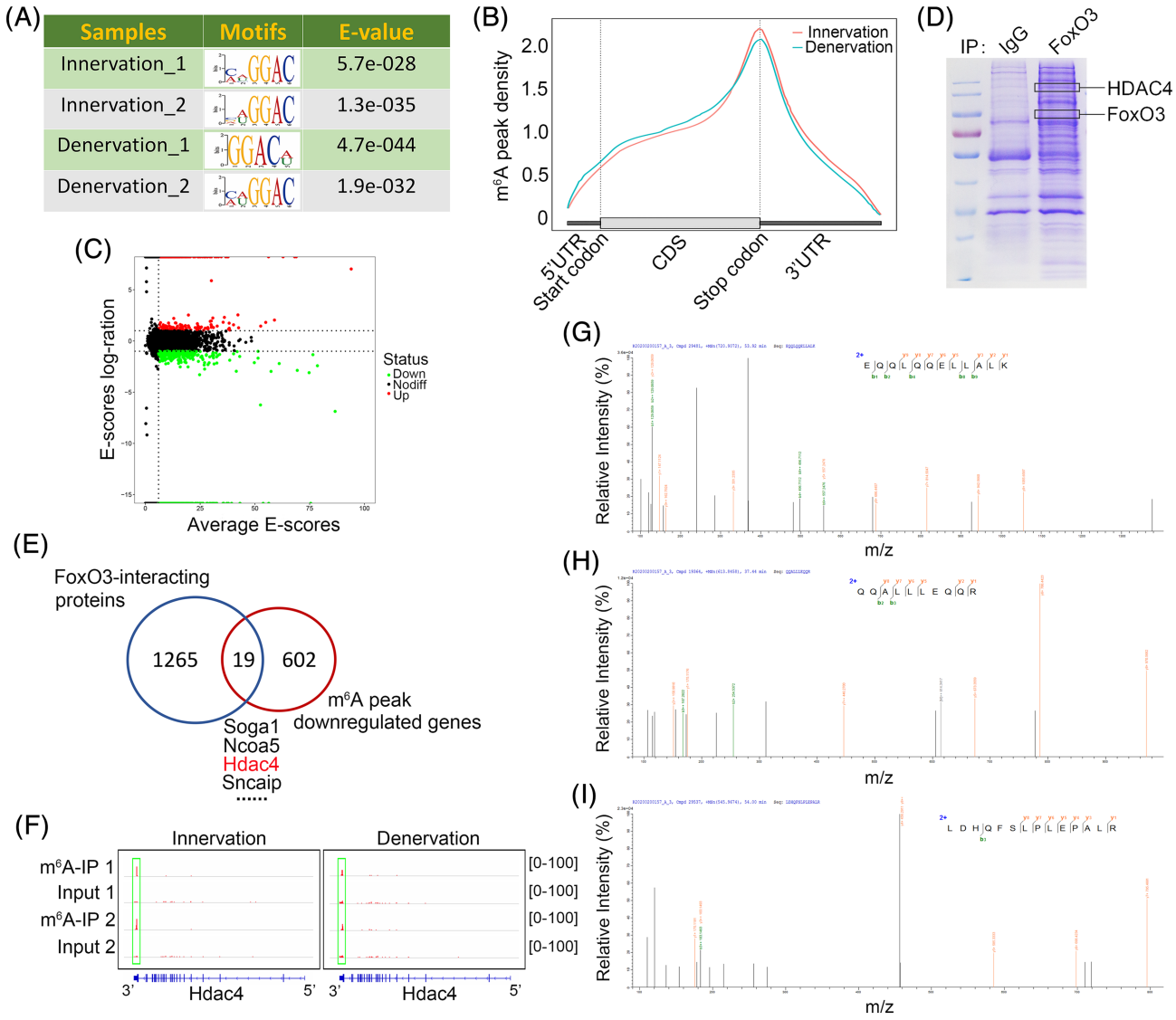

Figure 4 F Identification of m^{6}A targets in muscles undergoing denervation. (A) Motif analysis using MEME program identified 'GGAC' as the m^{6}A consensus motif in both the innervated and denervated muscles in m^{6}A-seq. (B) Density distribution of m^{6}A peaks across the transcriptome of gastrocnemius (GAS) muscle with innervation or denervation. (C) Scatter plots showing the distribution of m^{6}A peaks in the denervation group, compared with innervation group. (D) Coomassie staining of proteins co-immunoprecipitated with FoxO3 antibodies in denervated muscles. The marked bands were identified by tandem mass spectrometry (MS/MS). (E) Venn diagram showing overlap between FoxO3-interacting molecules and m6A-downregulated genes in GAS muscles with denervation. (F) Integrative genomics viewer (IGV) tracks displaying m^{6}A-seq read distribution in *Hdac4* transcript of innervated and denervated GAS muscles. (G–I) HDAC4 unique peptides (QQALLLEQQR; EQQLQQELLALK; LDHQFSLPLEPALR) identified by MS/MS analysis.

the literature and found that the function of FoxO3 protein in skeletal muscles is controlled by various post-translational modifications, such as phosphorylation, acetylation, methylation and ubiquitination.[25] This implies that ALKBH5 may indirectly affect FoxO3 protein levels by modulating specific post-translational modification molecule. To explore this postulate, co-immunoprecipitation (Co-IP) and tandem mass spectrometry analyses were performed. A total of 1284 FoxO3-interacting proteins were identified in denervated muscles (*Figure* 4D and 4E; *Table* S3). These proteins were crossed with differential genes of m^{6}A modification and 19 molecules overlapping between m^{6}A-downregulated genes and FoxO3-interacting proteins in denervated muscles were obtained (*Figure* 4E; *Table* S4). Among the 19 identified molecules, histone deacetylase 4 (HDAC4), a critical driver of skeletal muscle atrophy,[26,27] exhibited highly enriched and specific m^{6}A peaks near its stop codon and could interact with FoxO3 (*Figure* 4F–4I). These findings imply that HDAC4

may be the central mediator of ALKBH5-mediated regulation of FoxO3 expression.

ALKBH5-mediated m^{6}A demethylation is required for Hdac4 mRNA stability

The mechanism underlying the regulation of HDAC4 by ALKBH5 in skeletal muscles was investigated. ALKBH5 is a demethylase that selectively binds m^{6}A-containing RNA to regulate RNA splicing and stability[28,29]; therefore, expression levels of precursor (pre-) and mature mRNA of *Hdac4* were determined. Overexpressed ALKBH5 significantly increased the expression of mature *Hdac4* (*Figure* 5A), whereas *Alkbh5* knockout in denervated muscles significantly reduced mature *Hdac4* mRNA levels, compared with the control group (*Figure* 5B). There were no significant differences in *pre-Hdac4* levels between control and ALKBH5-modified muscles (*Figure* 5A and 5B), implying that *Hdac4* mRNA splicing was not affected by ALKBH5. Notably, alterations in mature *Hdac4* mRNA levels synchronously altered HDAC4 protein levels (*Figure* 5C and 5D). Then we determined whether ALKBH5 can affect the stability of *Hdac4* mRNA by overexpressing ALKBH5 *in vitro* through infection of C2C12 cells with Adv-ALKBH5, and used actinomycin D (Act-D) to block transcription. The half-life of mature *Hdac4* mRNA, but not *pre-Hdac4* mRNA was found to be significantly shorter in control cells, compared with ALKBH5-overexpressed cells (*Figure* 5E). These findings indicate that upregulated HDAC4 levels in dener-

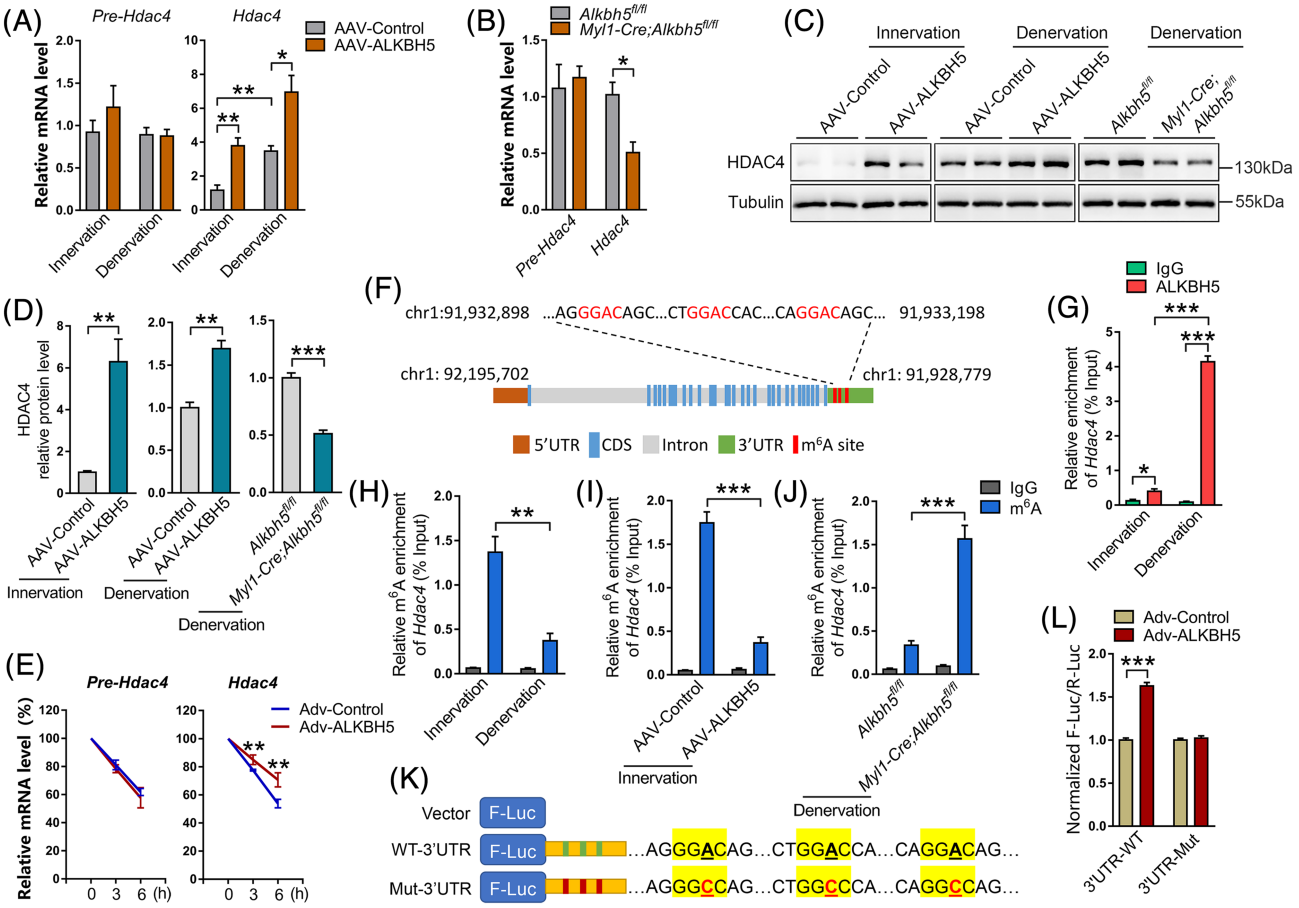

Figure 5 ALKBH5-mediated m^{6}A demethylation is required for *Hdac4* mRNA stability. (A) Precursor and mature mRNA levels of *Hdac4* in AAV-ALKBH5 infected muscle with or without denervation (n = 4). (B) Levels of *pre-Hdac4* and mature *Hdac4* in *Alkbh5* knockout muscle with denervation (n = 4). (C and D) Protein expression of HDAC4 in ALKBH5 overexpressed and *Alkbh5* knockout muscle with or without denervation (n = 4 or 6). (E) Half-life of *pre-Hdac4* and mature *Hdac4* mRNA at 0, 3, and 6 h after actinomycin D (5 μg/mL) treatment in C2C12 myotubes transduced with adenovirus expressing ALKBH5 (Adv-ALKBH5) (n = 4). (F) Schematic representation of positions of m^{6}A motifs within *Hdac4* mRNA. (G) CLIP-qPCR validation of ALKBH5 binding with 3′UTR of *Hdac4* mRNA in both innervated and denervated gastrocnemius (GAS) muscles (n = 4). (H) MeRIP-qPCR validation of m^{6}A changes in *Hdac4* mRNA in muscles during denervation (n = 4). (I and J) m^{6}A-MeRIP-qPCR showed that ALKBH5 overexpression depleted m^{6}A modification of *Hdac4* mRNA (I), whereas m^{6}A modification of *Hdac4* mRNA was enriched after ALKBH5 knockdown (J) (n = 4). (K) Schematic presentation for the generation of wild-type (WT) or three mutant (Mut; GGAC to GGCC) *Hdac4* 3′UTR firefly luciferase reporter. (L) Normalized F-Luc/R-Luc activity of the WT-3′UTR and three Mut-3′UTR reporter in Adv-ALKBH5 infected C2C12 cells (n = 6). Data are expressed as mean ± SEM. $^*P < 0.05$, $^{**}P < 0.01$, $^{***}P < 0.001$ by two-tailed Student's t test.

DOI: 10.1002/jcsm.12929

vated muscles can be attributed to ALKBH5-induced intensification of the stability of mature *Hdac4* mRNA.

To establish the precise mechanisms through which ALKBH5 increases *Hdac4* mRNA stability, m^6A sites were searched on *Hdac4* transcript based on m^6A-seq data. Three 'GGAC' motifs were identified near the stop codon in 3′UTR (*Figure* 5F), consistent with positions of peaks identified by m^6A-seq. Given that m^6A-seq showed that m^6A peak of *Hdac4* in 3′UTR significantly shrank with upregulation of ALKBH5 during denervation (*Figures* 1D, 1E and 4F), we conducted CLIP-qPCR assays using anti-ALKBH5 antibody in innervated and denervated muscles. We observed that ALKBH5 significantly enriched *Hdac4* transcripts (*Figure* 5G), implying that ALKBH5 regulates HDAC4 at RNA level. Then, we performed m^6A-MeRIP-qPCR using specific primers of these potential m^6A sites to verify ALKBH5-mediated m^6A demethylation in *Hdac4* mRNA. When compared with the IgG group, an obvious enrichment of *Hdac4* mRNA was obtained by reaction with m^6A-specific antibody (*Figure* 5H). Notably, either denervation or ALKBH5 overexpression remarkably reduced m^6A enrichment in the 3′UTR of *Hdac4* mRNA (*Figure* 5H and 5I), whereas deletion of *Alkbh5* caused an increase in m^6A levels in these sites (*Figure* 5J).

Thereafter, to investigate the essential roles of m^6A methylation in the *Hdac4* 3′UTR region, a luciferase reporter was generated with a wild-type (WT) *Hdac4*–3′UTR sequence or mutant (Mut) counterpart whose putative m^6A sites were mutated (GGAC to GGCC, *Figure* 5K). Co-transfection of ALKBH5 obviously increased expression levels of WT-3′UTR, but had no significant effects on the activity of Mut-3′UTR in C2C12 cells (*Figure* 5L). These findings indicate that ALKBH5-mediated m^6A demethylation on 3′UTR is involved in m^6A modification-regulated *Hdac4* expression.

Taken together, these findings show that ALKBH5 abrogates m^6A methylation at the 3′UTR region of *Hdac4* mRNA to inhibit m^6A-dependent mRNA degradation, which further increases the expression levels of HDAC4.

HDAC4 binds FoxO3 and enhances FoxO3 signalling via deacetylation

Mass spectrometry analysis showed that HDAC4 combines with FoxO3 in denervated muscles (*Figure* 4D, and 4G–4I). To further verify this finding, we investigated their interactions and colocalizations. Co-IP experiments revealed that HDAC4 and FoxO3 physically interacted with each other in denervated muscles (*Figure* 6A). Confocal microscopy showed that HDAC4 was colocalized with FoxO3 in muscle nucleus (*Figure* 6B). HDAC4 is a deacetylase; therefore, the role of HDAC4 in deacetylating FoxO3 in denervation-induced muscle atrophy was investigated. Upregulation of HDAC4 was correlated with a significant decrease in acetylated FoxO3 proteins immunoprecipitated with an antibody against acetylated-lysine (Ace-lys) after denervation, compared with the control group (*Figure* 6C). This finding implies that HDAC4 can remove acetylation modification on FoxO3. To verify that FoxO3 is a deacetylation substrate of HDAC4, Myc-tagged HDAC4 and Flag-tagged FoxO3 were expressed in HEK293T. Co-IP experiments showed that exogenous HDAC4 strongly interacted with exogenous FoxO3, thereby reducing the acetylation levels of FoxO3 (*Figure* 6D).

Deacetylation is capable of increasing FoxO3 protein levels by protecting it against ubiquitination-mediated degradation.[30] Therefore, we first determined whether HDAC4-mediated deacetylation regulates FoxO3 protein levels. Western blot showed that ectopic expression of HDAC4 significantly increased the protein levels of exogenous FoxO3 in a dose-dependent manner (*Figure* 6E). Meanwhile, HDAC4 promoted endogenous FoxO3 protein levels (*Figure* 6F). In contrast, promotion of FoxO3 protein levels by HDAC4 was blocked by treatment with LMK-235, an inhibitor of HDAC4 (*Figure* 6G). Second, to ascertain the effects of HDAC4 on the stability of FoxO3 proteins, turnover rate of FoxO3 in the presence or absence of HDAC4 was determined using the protein synthesis inhibitor cycloheximide (CHX). Transfection of HDAC4 expression plasmid in NIH/3T3 cells remarkably prolonged the half-life of both exogenous and endogenous FoxO3, compared with the empty vector (*Figure* 6H and 6I), suggesting that HDAC4 specifically stabilized FoxO3 in cells. Third, to confirm the role of HDAC4 in preventing FoxO3 ubiquitination degradation, Myc-HDAC4, Flag-FoxO3, and HA-Ubiquitin expression vectors were transfected into HEK293T cells, followed by treatment with LMK-235 or DMSO. FoxO3 ubiquitination was greatly suppressed by HDAC4 (lane 3), compared with the control vector (lane 2), while inhibition of HDAC4 by LMK-235 elevated FoxO3 ubiquitylation levels (lane 4) (*Figure* 6J). Consistently, inhibitory effects of HDAC4 on FoxO3 ubiquitination degradation were observed *in vivo* (*Figure* 6K).

Given that deacetylation is necessary for activation of FoxO3,[31] we assessed the effects of HDAC4-mediated deacetylation on FoxO3 transcriptional activities using a FoxO sensor that contained six FoxO DNA-binding elements (DBE reporter) upstream of the luciferase gene.[32] Overexpressed HDAC4 elevated luciferase reporter activities, compared with the empty vector, whereas luciferase activities were significantly suppressed after LMK-235 addition (*Figure* 6L). Similar findings were observed when the transfection of *Atrogin1* or *MuRF1* promoters controlled luciferase reporter (*Figure* 6M and 6N).

These findings demonstrate that HDAC4-mediated deacetylation serves as a switch to control the ubiquitination levels of FoxO3, thereby modulating protein expressions and transcriptional activities of FoxO3 in skeletal muscles.

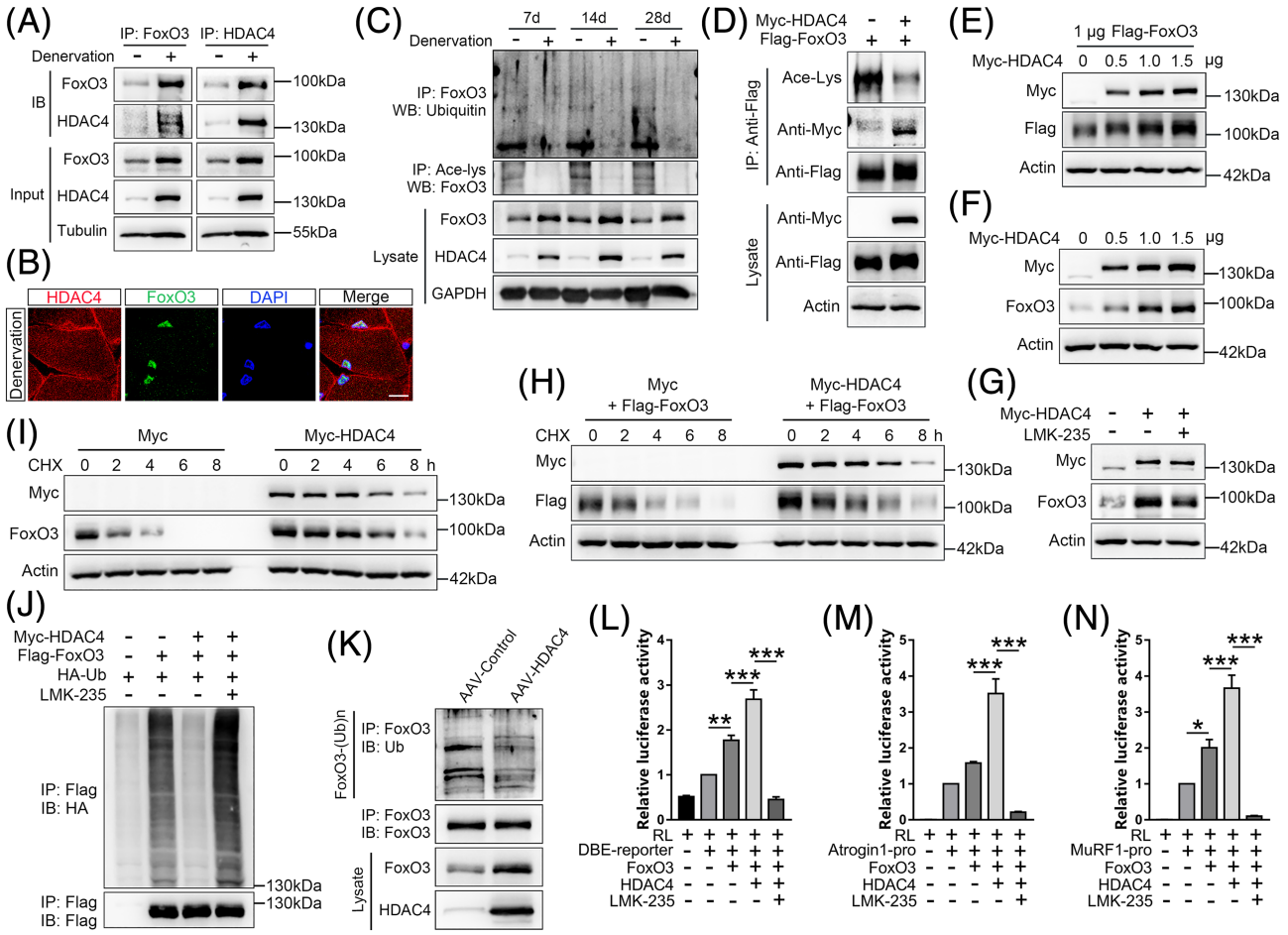

Figure 6 HDAC4 binds FoxO3 and enhances FoxO3 signalling by deacetylation. (A) HDAC4 endogenously interacts with FoxO3 in denervated muscles as shown by co-immunoprecipitation (Co-IP) with FoxO3 (left) or HDAC4 (right) antibody. (B) Confocal images showing colocalization between HDAC4 (red) and FoxO3 (green) in the nucleus (blue, DAPI-labelled) of gastrocnemius (GAS) muscles after 14 days of denervation. Scale bar = 10 μm. (C) Co-IP and immunoblot showing decrease in acetylation and ubiquitination levels of FoxO3 proteins in GAS muscles on Days 7, 14, and 28 post-denervation. (D) Immunoblot analysis with anti-Ace-Lys, anti-Myc, and anti-Flag for proteins that co-immunoprecipitated with Flag-tagged FoxO3 from lysates of HEK293T cells that were transfected with plasmids encoding the proteins indicated in the above blots. (E and F) Increasing amounts of Myc-HDAC4 expression plasmid were transfected into NIH/3T3 cells with or without Flag-FoxO3 plasmid (1 μg). Exogenous (E) and endogenous (F) protein levels of FoxO3 were determined by immunoblotting with a specific antibody 24 h after transfection. (G) NIH/3T3 cells were transfected with Myc-HDAC4 plasmid (1 μg), followed by LMK-235 (2 μM) treatment for 12 h. Endogenous protein levels of FoxO3 were then determined. (H and I) Myc-HDAC4 plasmid (1 μg) was transfected into NIH/3T3 cells together with or without Flag-FoxO3 plasmid (1 μg), and cells were treated with cycloheximide (CHX) at 80 μg/mL for the indicated times. Half-life of exogenous (H) and endogenous (I) FoxO3 proteins were determined by western blot. (J) HEK293T cells transfected with plasmids were treated with LMK-235 (2 μM, 12 h) and proteasome inhibitor MG132 (20 μM, 8 h). Polyubiquitination of exogenous FoxO3 was detected by anti-HA antibodies. (K) TA muscles were infected with AAV-HDAC4 for 6 weeks. Endogenous FoxO3 was immunoprecipitated with anti-FoxO3, and its polyubiquitination detected by anti-Ubiquitin (Ub). (L–N) Relative luciferase activities of DBE (L), *Atrogin1*-pro (M) or *MuRF1*-pro (N) reporter in C2C12 cells that had been transfected with Myc-HDAC4, Flag-FoxO3 and RL reporter (n = 6 or 8). Data are expressed as mean ± SEM. $^{**}P < 0.01$, $^{***}P < 0.001$ by one-way ANOVA with Bonferroni's post-hoc test.

HDAC4 reversed the regulatory effects of ALKBH5 on muscle mass

To confirm that ALKBH5-induced muscle mass loss was mediated by HDAC4, first, we inhibited HDAC4 by intraperitoneal injection of LMK-235 in AAV-ALKBH5-infected mice. LMK-235 injection significantly elevated acetyl-Histone H3 levels, indicating that HDAC4 activities were successfully suppressed (*Figure* 7F and 7G). In addition, improved muscle weight and myofibre CSA were observed after LMK-235 injection in ALKBH5-induced muscle atrophy model (*Figure* 7A–7E). Notably, western blot showed that inhibition of HDAC4 significantly upregulated MyHC while significantly downregulating FoxO3 levels (*Figure* 7F and 7G). Further, we transfected AAV-HDAC4 or AAV-Control into TA muscles of *Myl1-Cre*;

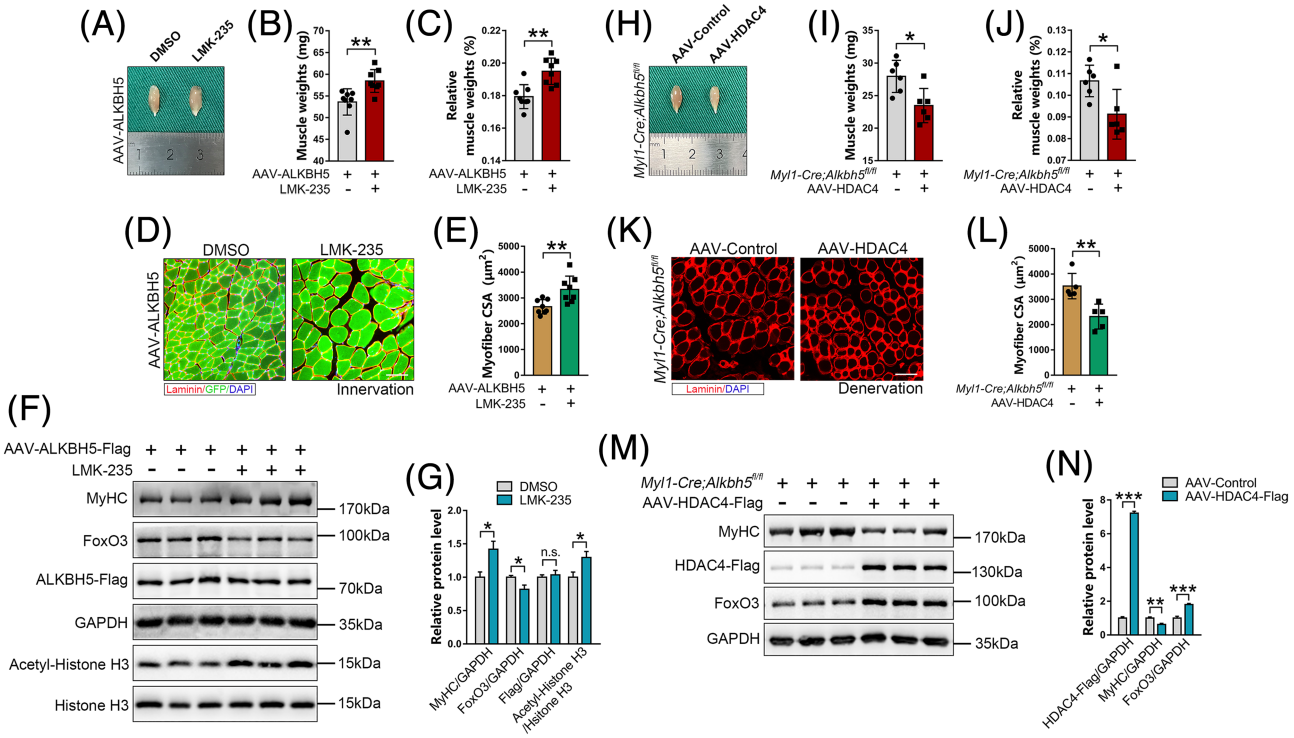

Figure 7 HDAC4 reversed the regulatory effects of ALKBH5 on muscle mass. (A–E) The wet weight (B), percentage of muscle wet weight relative to body weight (C), and myofibre cross-sectional area (CSA) (E) of ALKBH5-overexpressed TA muscles after 14 days of LMK-235 injection (5 mg/kg/day) (n = 8). Scale bar = 100 μm. (F and G) Protein levels of MyHC, FoxO3, ALKBH5-Flag, and acetyl-Histone H3 in ALKBH5-overexpressed TA muscle after 14 days of LMK-235 injection (n = 5). GAPDH and Histone H3 were used as internal controls. (H–L) TA muscle wet weight (I), percentage of muscle wet weight relative to body weight (J), and myofibre CSA (L) of *Alkbh5* knockout mice after 4 weeks of AAV-HDAC4 infection, followed by 21 days of denervation (n = 5 or 6). Scale bar = 100 μm. (M and N) Protein levels of MyHC, FoxO3, and HDAC4-Flag in *Alkbh5* knockout TA muscles after 4 weeks of AAV-HDAC4 infection, followed by 21 days denervation (n = 6). Data are expressed as mean ± SD (B, C, E, I, J, L) or mean ± SEM (G, N). $^{*}P < 0.05$, $^{**}P < 0.01$, $^{***}P < 0.001$ by two-tailed Student's t test.

Alkbh5$^{fl/fl}$ mice and established denervation-induced muscle atrophy model. Overexpression of HDAC4 reversed the protective effects of *Alkbh5* knockout on muscle wasting, as indicated by reduction of muscle weight and CSA, downregulation of MyHC, and increase in FoxO3 expression (*Figure* 7H–7N). These findings show that HDAC4 is a vital mediator and its suppression can partially rescue the effect of ALKBH5 in promoting skeletal muscle atrophy.

Discussion

Previous studies report that m^{6}A modification in eukaryotic RNA regulates physiological homeostasis and development of diseases.[13–16] In skeletal muscles, a strong and intricate relationship between m^{6}A modification and myogenesis has been documented. Dysregulation of m^{6}A decreases MyoD expression in proliferative myoblasts, disrupts the specification and differentiation of myoblasts into myotubes,[17] suppresses mitochondrial biogenesis and energy production during muscle development.[18] We investigated the function of m^{6}A on muscle phenotypes in adults. It was established that m^{6}A regulates adult skeletal muscle mass and size, especially in denervation-induced muscle atrophy. The m^{6}A mRNA levels of skeletal muscles undergoing denervation significantly decreased, compared with control muscles. Moreover, expressions of m^{6}A demethylase ALKBH5 was upregulated in denervated muscles. Overexpressed ALKBH5 reduced wet weight and fibre CSA in innervated and denervated muscles, whereas deletion of *Alkbh5* protected mice against denervation-induced muscle wasting with no effects on physical development and normal muscle morphologies. Even though studies have documented the biological and pathological roles of ALKBH5 in autophagy,[33] spermatogenesis,[29] ossification,[34] and cancer,[35] we, for the first time, proved the crucial function of ALKBH5 in controlling muscle mass in adults. Importantly, given the high feasibility and operability of developing drugs targeting enzyme protein, m^{6}A demethylase ALKBH5 is a potential target for preventing neurogenic muscle atrophy.

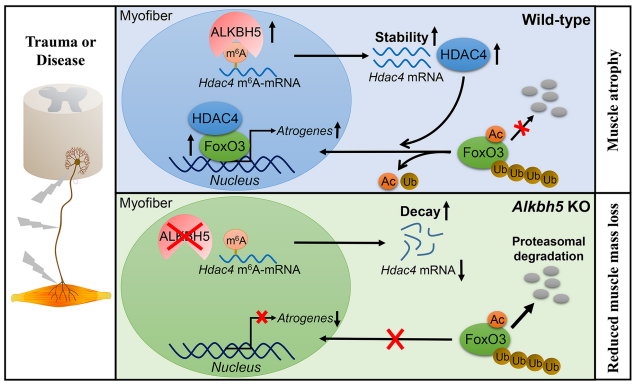

Figure 8 Schematic illustration of ALKBH5-HDAC4-FoxO3 axis promoting denervation-induced muscle atrophy. In denervated muscles, ALKBH5-mediated m^{6}A demethylation stabilized and increased HDAC4 expression. HDAC4 interacted with FoxO3 and inhibited its degradation in a deacetylation-dependent manner, ultimately leading to an increase in FoxO3 protein levels and transcriptional activities. Targeting ALKBH5 reduced HDAC4 levels, which in turn suppressed FoxO3 signalling activation and prevented denervation-induced muscle atrophy.

FoxO3 is a transcription factor that is implicated in atrogene expression and muscle wasting in various pathological conditions, including denervation.[6–8] The findings of this study showed that ALKBH5 positively regulated the expressions of FoxO3 proteins during denervation, suggesting that FoxO3 may be a downstream molecule of ALKBH5. Then, m^{6}A-seq and FoxO3 co-immunoprecipitation combined with mass spectrometry analyses were performed. The findings showed that FoxO3 is not a direct target for ALKBH5-mediated m^{6}A modification, however, it is indirectly regulated by the 'bridge' molecule HDAC4.

In this study, HDAC4 was identified as a novel substrate for ALKBH5 in denervated muscles. ALKBH5 improved mRNA stability of HDAC4 transcripts, leading to increased HDAC4 expressions through an m^{6}A demethylation-dependent mechanism. Regulation of mRNA stability is an important mechanism through which m^{6}A modification affects gene expression. The diversity in cell type and state results in differences in effects of ALKBH5-mediated m^{6}A demethylation on mRNA stability. On the one hand, ALKBH5 demethylates and stabilizes *PER1* mRNA and prevents pancreatic cancer progression.[36] ALKBH5 promotes cancer stem cell self-renewal in acute myeloid leukaemia by abolishing m^{6}A-dependent *TACC3* mRNA degradation.[37] On the other hand, ALKBH5 decreases the stability of *CYR61* mRNA and inhibits trophoblast invasion at the maternal–foetal interface.[38] Overexpression of ALKBH5 can shorten the half-life of *LYPD1* mRNA and suppress the proliferation and metastasis of hepatocellular carcinoma.[39] In our study, we found that ALKBH5 enhances the stability of *Hdac4* mRNA through m^{6}A demethylation at the 3′UTR, which further increases its expression level in denervated muscles (*Figure* 8). Therefore, ALKBH5 is a novel mechanism for upregulating HDAC4 levels in denervation-induced muscle atrophy.

Prevention of overactivation of FoxO3 signalling is essential to avoid muscle wasting. Actually, FoxO3 is regulated by many different post-translational modifications, including acetylation/deacetylation and ubiquitination.[5] Acetyltransferase or deacetylase can negatively or positively modulate FoxO3 activities in skeletal muscles. For instance, p300/CBP-mediated acetylation of FoxO3 suppresses its nuclear localization and makes it inactive in denervation-induced muscle atrophy.[40] In addition, HDAC1-mediated deacetylation activates FoxO3-dependent atrophy during nutrient deprivation.[31] Although HDAC4 is involved in deacetylation and activation of FoxO3 in vascular endothelial cells,[41] the specific proteins mediating FoxO3 deacetylation in muscles undergoing denervation have not been identified. This study proves, for the first time, that HDAC4 directly deacetylates FoxO3 in skeletal muscles and is necessary for its upregulation and activation in response to denervation (*Figure* 8).

Of cause, there are some weaknesses in this study to ameliorate by future works. First, in consideration of the easy transfection of HEK293T and NIH/3T3 cells, we used these two non-muscle cells rather than myocyte/myotube models to explore the regulatory relationship between HDAC4 and FoxO3. Second, if we use HDAC4 constructs deficient in enzyme activity instead of chemical inhibitor, the results may be more convincing. These weaknesses are also the area of interest for our future investigation.

In summary, through analysis of regulatory relationships among ALKBH5, HDAC4, and FoxO3, we revealed that ALKBH5 demethylates and stabilizes *Hdac4*, leading to upregulation and activation of FoxO3, which accelerates denervation-induced muscle wasting. Our findings elucidate on the pivotal regulatory role of m^{6}A in muscle health and diseases and shed light on the development of new therapeutic strategies for neurogenic muscle atrophy.

Acknowledgements

This work was supported by the National Natural Science Foundation of China (No. 32100915), Shenzhen Municipal Science and Technology Innovation Committee Project (SGLH20180625141602256, JCYJ20180305164544288, JSGG20180504170427135, JCYJ20190807145011340), and Guangdong Basic and Applied Basic Research Foundation (2019A1515110402). The authors of this manuscript certify that they comply with the ethical guidelines for authorship and publishing in the *Journal of Cachexia, Sarcopenia and Muscle*.[42]

Online supplementary material

Additional supporting information may be found online in the Supporting Information section at the end of the article.

Conflict of interest

The authors declare that they have no conflict of interest.

References

1. Ehmsen JT, Höke A. Cellular and molecular features of neurogenic skeletal muscle atrophy. *Exp Neurol* 2020;**331**:113379.
2. Vainshtein A, Sandri M. Signaling pathways that control muscle mass. *Int J Mol Sci* 2020;**21**:4759.
3. Liu H, Thompson LV. Skeletal muscle denervation investigations: selecting an experimental control wisely. *Am J Physiol Cell Physiol* 2019;**316**:C456–C461.
4. Furrer R, Handschin C. Muscle wasting diseases: novel targets and treatments. *Annu Rev Pharmacol Toxicol* 2019;**59**:315–339.
5. Sartori R, Romanello V, Sandri M. Mechanisms of muscle atrophy and hypertrophy: implications in health and disease. *Nat Commun* 2021;**12**:330.
6. Milan G, Romanello V, Pescatore F, Armani A, Paik JH, Frasson L, et al. Regulation of autophagy and the ubiquitin-proteasome system by the FoxO transcriptional network during muscle atrophy. *Nat Commun* 2015;**6**:6670.
7. Rom O, Reznick AZ. The role of E3 ubiquitin-ligases MuRF-1 and MAFbx in loss of skeletal muscle mass. *Free Radic Biol Med* 2016;**98**:218–230.
8. O'Neill BT, Bhardwaj G, Penniman CM, Krumpoch MT, Suarez Beltran PA, Klaus K, et al. FoxO transcription factors are critical regulators of diabetes-related muscle atrophy. *Diabetes* 2019;**68**:556–570.
9. Zhang W, Zhang S, Yan P, Ren J, Song M, Li J, et al. A single-cell transcriptomic landscape of primate arterial aging. *Nat Commun* 2020;**11**:2202.
10. Calissi G, Lam EW, Link W. Therapeutic strategies targeting FOXO transcription factors. *Nat Rev Drug Discov* 2021;**20**:21–38.
11. Lan Q, Liu PY, Haase J, Bell JL, Hüttelmaier S, Liu T. The critical role of RNA m^6A methylation in cancer. *Cancer Res* 2019;**79**:1285–1292.
12. Shi H, Wei J, He C. Where, when, and how: context-dependent functions of RNA methylation writers, readers, and erasers. *Mol Cell* 2019;**74**:640–650.
13. Zhang M, Zhai Y, Zhang S, Dai X, Li Z. Roles of N^6-methyladenosine (m^6A) in stem cell fate decisions and early embryonic development in mammals. *Front Cell Dev Biol* 2020;**8**:782.
14. Wang CX, Cui GS, Liu X, Xu K, Wang M, Zhang XX, et al. METTL3-mediated m^6A modification is required for cerebellar development. *PLoS Biol* 2018;**16**:e2004880. https://doi.org/10.1371/journal.pbio.2004880
15. Dorn LE, Lasman L, Chen J, Xu X, Hund TJ, Medvedovic M, et al. The N(^{6})-methyladenosine mRNA methylase METTL3 controls cardiac homeostasis and hypertrophy. *Circulation* 2019;**139**:533–545.
16. Wang T, Kong S, Tao M, Ju S. The potential role of RNA N6-methyladenosine in cancer progression. *Mol Cancer* 2020;**19**:88.
17. Kudou K, Komatsu T, Nogami J, Maehara K, Harada A, Saeki H, et al. The requirement of Mettl3-promoted MyoD mRNA maintenance in proliferative myoblasts for skeletal muscle differentiation. *Open Biol* 2017;**7**:170119, https://doi.org/10.1098/rsob.170119
18. Wang X, Huang N, Yang M, Wei D, Tai H, Han X, et al. FTO is required for myogenesis by positively regulating mTOR-PGC-1alpha pathway-mediated mitochondria biogenesis. *Cell Death Dis* 2017;**8**:e2702, https://doi.org/10.1038/cddis.2017.122
19. Zhang S, Zhao BS, Zhou A, Lin K, Zheng S, Lu Z, et al. m^6A demethylase ALKBH5 maintains tumorigenicity of glioblastoma stem-like cells by sustaining FOXM1 expression and cell proliferation program. *Cancer Cell* 2017;**31**:591–606.
20. Hao L, Yin J, Yang H, Li C, Zhu L, Liu L, et al. ALKBH5-mediated m^6A demethylation of FOXM1 mRNA promotes progression of uveal melanoma. *Aging* 2021;**13**:4045–4062.
21. Zeng Y, Wang S, Gao S, Soares F, Ahmed M, Guo H, et al. Refined RIP-seq protocol for epitranscriptome analysis with low input materials. *PLoS Biol* 2018;**16**:e2006092, https://doi.org/10.1371/journal.pbio.2006092
22. Liu Y, Li J, Shang Y, Guo Y, Li Z. CARM1 contributes to skeletal muscle wasting by mediating FoxO3 activity and promoting myofiber autophagy. *Exp Cell Res* 2019;**374**:198–209.
23. Goto-Inoue N, Morisasa M, Machida K, Furuichi Y, Fujii NL, Miura S, et al. Characterization of myofiber-type-specific molecules using mass spectrometry imaging. *Rapid Commun Mass Spectrom* 2019;**33**:185–192.
24. Zhang Y, Wang X, Zhang X, Wang J, Ma Y, Zhang L, et al. RNA-binding protein YTHDF3 suppresses interferon-dependent antiviral responses by promoting FOXO3 translation. *Proc Natl Acad Sci U S A* 2019;**116**:976–981.
25. Tia N, Singh AK, Pandey P, Azad CS, Chaudhary P, Gambhir IS. Role of Forkhead Box O (FOXO) transcription factor in aging and diseases. *Gene* 2018;**648**:97–105.
26. Moresi V, Williams AH, Meadows E, Flynn JM, Potthoff MJ, McAnally J, et al. Myogenin and class II HDACs control neurogenic muscle atrophy by inducing E3 ubiquitin ligases. *Cell* 2010;**143**:35–45.
27. Luo L, Martin SC, Parkington J, Cadena SM, Zhu J, Ibebunjo C, et al. HDAC4 controls muscle homeostasis through deacetylation of myosin heavy chain, PGC-1α, and Hsc70. *Cell Rep* 2019;**29**:749–763.
28. Zhang C, Samanta D, Lu H, Bullen JW, Zhang H, Chen I, et al. Hypoxia induces the breast cancer stem cell phenotype by HIF-dependent and ALKBH5-mediated m^6A-demethylation of NANOG mRNA. *Proc Natl Acad Sci U S A* 2016;**113**:E2047–E2056.
29. Tang C, Klukovich R, Peng H, Wang Z, Yu T, Zhang Y, et al. ALKBH5-dependent m^6A demethylation controls splicing and stability of long 3′-UTR mRNAs in male germ cells. *Proc Natl Acad Sci U S A* 2018;**115**:E325–E333.
30. Tseng AH, Wu LH, Shieh SS, Wang DL. SIRT3 interactions with FOXO3 acetylation, phosphorylation and ubiquitinylation mediate endothelial cell responses to hypoxia. *Biochem J* 2014;**464**:157–168.
31. Beharry AW, Sandesara PB, Roberts BM, Ferreira LF, Senf SM, Judge AR. HDAC1 ac-

tivates FoxO and is both sufficient and required for skeletal muscle atrophy. *J Cell Sci* 2014;**127**:1441–1453.
32. Furuyama T, Kitayama K, Yamashita H, Mori N. Forkhead transcription factor FOXO1 (FKHR)-dependent induction of PDK4 gene expression in skeletal muscle during energy deprivation. *Biochem J* 2003;**375**:365–371.
33. Song H, Feng X, Zhang H, Luo Y, Huang J, Lin M, et al. METTL3 and ALKBH5 oppositely regulate m^6A modification of *TFEB* mRNA, which dictates the fate of hypoxia/reoxygenation-treated cardiomyocytes. *Autophagy* 2019;**15**:1419–1437.
34. Wang HF, Kuang MJ, Han SJ, Wang AB, Qiu J, Wang F, et al. BMP2 modified by the m^6A demethylation enzyme ALKBH5 in the ossification of the ligamentum flavum through the AKT signaling pathway. *Calcif Tissue Int* 2020;**106**:486–493.
35. Wang J, Wang J, Gu Q, Ma Y, Yang Y, Zhu J, et al. The biological function of m^6A demethylase ALKBH5 and its role in human disease. *Cancer Cell Int* 2020;**20**:347.
36. Guo X, Li K, Jiang W, Hu Y, Xiao W, Huang Y, et al. RNA demethylase ALKBH5 prevents pancreatic cancer progression by posttranscriptional activation of PER1 in an m^6A-YTHDF2-dependent manner. *Mol Cancer* 2020;**19**:91.
37. Shen C, Sheng Y, Zhu AC, Robinson S, Jiang X, Dong L, et al. RNA demethylase ALKBH5 selectively promotes tumorigenesis and cancer stem cell self-renewal in acute myeloid leukemia. *Cell Stem Cell* 2020;**27**:64–80.
38. Li XC, Jin F, Wang BY, Yin XJ, Hong W, Tian FJ. The m^6A demethylase ALKBH5 controls trophoblast invasion at the maternal-fetal interface by regulating the stability of *CYR61* mRNA. *Theranostics* 2019;**9**:3853–3865.
39. Chen Y, Zhao Y, Chen J, Peng C, Zhang Y, Tong R, et al. ALKBH5 suppresses malignancy of hepatocellular carcinoma via m^6A-guided epigenetic inhibition of LYPD1. *Mol Cancer* 2020;**19**:123.
40. Bertaggia E, Coletto L, Sandri M. Posttranslational modifications control FoxO3 activity during denervation. *Am J Physiol Cell Physiol* 2012;**302**:C587–C596.
41. Yang D, Xiao C, Long F, Su Z, Jia W, Qin M, et al. HDAC4 regulates vascular inflammation via activation of autophagy. *Cardiovasc Res* 2018;**114**:1016–1028.
42. von Haehling S, Morley JE, Coats AJS, Anker SD. Ethical guidelines for publishing in the Journal of Cachexia, Sarcopenia and Muscle: update 2019. *J Cachexia Sarcopenia Muscle* 2019;**10**:1143–1145.